Available online at www.sciencedirect.com
SCIENCE DIRECT®
Biosensors and Bioelectronics 20 (2005) 1366–1372
BIOSENSORS & BIOELECTRONICS
www.elsevier.com/locate/bios

Selective glucose detection based on the concept of electrochemical depletion of electroactive species in diffusion layer

Kang Wang, Jing-Juan Xu, Da-Cheng Sun, Hui Wei, Xing-Hua Xia*

The State Key Laboratory of Coordination Chemistry, Department of Chemistry, Institute of Analytical Science, Nanjing University, Nanjing 210093, China

Received 24 February 2004; received in revised form 22 May 2004; accepted 31 May 2004
Available online 2 July 2004

Abstract

A glucose detection approach based on the concept of electrochemical depletion of electroactive species in diffusion layer was established, using scanning electrochemical microscopy (SECM). By controlling the glucose oxidase (GOD) modified electrode (substrate electrode) at a proper potential of electrochemical oxidation of interfering electroactive species, i.e., ascorbic acid (AA), an interference-free microcircumstance was formed in the diffusion layer of the substrate electrode. Consequently, we could successfully sense hydrogen peroxide generated from an enzymatic reaction by locating a Pt ultramicroelectrode (UME) (tip electrode, 5 μm in radius) into the diffusion layer of the substrate electrode. Properties of this interference-removing approach based on electrochemical depletion were systematically investigated. Results showed that the interference-removing efficiency was significantly determined by the tip-substrate distance and substrate potential. When the tip-substrate distance was 11 μm (2.2 times of the tip electrode radius) and the substrate potential was 0.5 V, nearly 90% of AA (0.5 mM) could be depleted within 30 s without consumption of H_2O_2. Under these conditions, 0.1 mM AA showed no influence on the detection of 0.5 mM glucose. The linear range of glucose detection is 0.01–1 mM with a detection limit (DL) of 0.005 mM (correlation coefficient is 0.9948). This research will open a new way for developing selective micro-biosensors.

Keywords: Biosensor; Glucose detection; Diffusion layer; Electrochemical depletion; SECM; Selectivity

1. Introduction

Electrochemical method has been widely applied in biochemical analysis for its advantages of simplicity and sensitivity (Mello and Kubota, 2002; Gerard et al., 2002). In electrochemical sensing devices, redox enzyme is usually immobilized on a working electrode to provide specific response to its substrate. Glucose oxidase (GOD) based biosensors attracted considerable interests for the importance of glucose in clinical and food analysis (Wang, 2001). Although, the oxidation of glucose by means of the catalytic activity of GOD is highly specific, the detection principle of a glucose sensor itself—the usually amperometric detection of the formed hydrogen peroxide, is largely unspecific. Therefore, such electrochemical sensors are highly sensitive towards side reaction caused by chemical impurities, such as ascorbic acid (AA). Various studies have been done to improve the applicability of GOD-based sensors by overcoating a permselective membrane onto the enzyme-immobilizing layer, by using electron-carrying mediators or by direct electron transfer between enzyme and electrode. (Wang, 2001; Zhang et al., 1994; Myler et al., 2002; Xiao et al., 2003). Nevertheless, these methods will either inhibit diffusion of glucose into the modified enzyme layer or reduce the activity of immobilized GOD. Furthermore, the leakage of mediator molecules or the non-uniformity of overcoated membranes made the interference-removing capability change with performance time or vary in batches.

It is one of our long-term goals to develop simple and stable interference-removing approaches that could be used in micro-electrochemical devices. We realize that electrochemical depletion of reactive species is a reproducible and easy-controlled approach to improve the applicability of biosensors. Electrochemical depletion approach has high

* Corresponding author. Tel.: +86 25 83597436; fax: +86 25 83597436.
E-mail address: xhxia@nju.edu.cn (X.-H. Xia).

0956-5663/$ – see front matter © 2004 Elsevier B.V. All rights reserved.
doi:10.1016/j.bios.2004.05.009

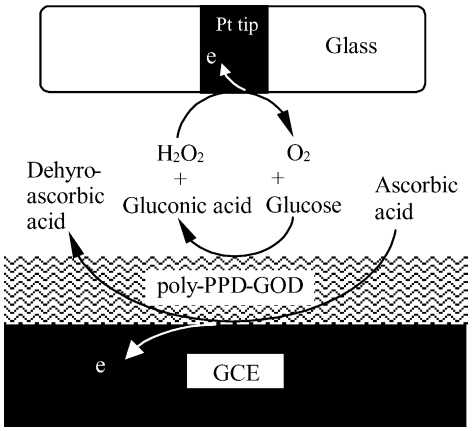

Fig. 1. Scheme and principle of the glucose detection and interference-removing approach in the diffusion layer of GOD-modified GCE.

interference-removing ability in the diffusion layer and it is suitable for the fabrication of micro-electrochemical detectors. In this paper, a selective glucose detection system based on the concept of electrochemical depletion of electroactive species in diffusion layer was established. As shown in Fig. 1, a macro glassy carbon electrode (GCE) immobilized with GOD was polarized to a potential at which interference species could be electrochemically depleted. Thus, an interference-free micro-circumstance was created in the diffusion layer of the GCE. A tip electrode was located into this diffusion layer to detect glucose by sensing H_2O_2 that formed in the enzymatic reaction (Eq. (1)):

$$\beta\text{-D-glucose} + O_2 \xrightarrow{\text{GOD}} \text{gluconic acid} + H_2O_2 \quad (1)$$

Glucose detection based on the concept of diffusion layer provides a new way for developing high selective biosensors with two closely positioned working electrodes. Though Lunte (Lunte et al., 1987) has used dual-electrode to investigate voltammetric detection in a flow-through thin-layer electrochemical cell and found that any reactions at an upstream electrode reducing the concentration of the analyte in the mobile phase would cause a decrease in the current at a downstream electrode, their detection approach is in essence a bulk pre-oxidation approach. To our knowledge, quantitative investigations of electrochemical depletion of reactive species in the diffusion layer have not been reported.

Scanning electrochemical microscopy (SECM) is a scanning probe microscopic technique that explores chemical information of a specimen (substrate) surface by positioning an ultramicroelectrode (UME, the tip electrode) a few micrometers above the substrate in nanometer precision (Kwak and Bard, 1989; Bard et al., 1989). When the tip electrode is positioned far from the substrate (in the bulk solution), its diffusion-controlled current can be defined by a UME equation (Eq. (2)),

$$i_{T,\infty} = 4nFDca \quad (2)$$

where c, D and n are, respectively, the bulk concentration, the diffusion coefficient, and the number of electrons in the electrochemical reaction; a is the electrode radius and F the Faraday constant. When the tip is near the substrate, electric communication between them occurs, resulting in an increase (for conductive or reactive surface) or a decrease (for insulating or non-reactive surface) in tip current (Kwak and Bard, 1989). The distance between the tip and the specimen can be calculated conveniently according to the change of tip current (Amphlett and Denuault, 1998). Previous studies have proved that SECM is a powerful tool for obtaining spatial resolved chemical information of the biological materials (Kasai et al., 2000; Liebetrau et al., 2003). For the investigation of enzyme-contained system, SECM has been used to characterize the enzyme-modified surfaces or enzyme patterns (Zhou et al., 2002; Kasai et al., 2002; Gaspar et al., 2001; Turyan et al., 2000; Pierce et al., 1992). Therefore, SECM could give a convenient spatial control in the diffusion layer for this research. The influence of substrate potential, the tip-substrate distance on glucose detection and interference-removing efficiency were systematically investigated.

2. Experimental section

2.1. Chemicals and materials

GOD (Catalog No. G7773, EC 1.1.3.4, type II from *Aspergillus niger*, 15, 500 units/g, Sigma) was used as received. Potassium ferrocyanide, glucose and *p*-phenylenediamine (PPD) were of analytical grade (Nanjing, China). GOD was dissolved in 50 mM phosphate buffer solution (PBS, pH 7.4) containing 100 mM KCl. All solutions were prepared with 18.2 MΩ deionized water (Purelab Classic Corp., USA).

2.2. SECM system

A model CHI 900 SECM (CH Instruments, Austin, TX) was used for the measurement of SECM images and approach curves. The SECM tip was a Pt (tip radius $r_T = 5\,\mu m$; insulating glass outer wall radius r_{glass}: $r_T = 10$) UME (CH Instruments). All electrochemical measurements were performed in a Teflon cell (ca. 1.5 ml). Four-electrode system was used for all measurements with a Pt wire as counter electrode, an Ag/AgCl (in 3 M KCl) as reference electrode, and the Pt tip as the first working electrode. A GOD layer modified glassy carbon disk electrode (GCE, 3.5 mm in diameter) was used as both the second working electrode and the substrate of SECM. Before each measurement, the Pt UME was polished with 0.05 μm alumina slurry on microcloth pads. The SECM tip electrode was then precisely positioned at a predetermined distance from the sample surface by monitoring the anodic current at 0.5 V for the electrochemical oxidation of 1 mM $Fe(CN)_6^{4-}$ and then comparing the measured anodic current with the normalized current-distance curve

for SECM negative feedback behavior. After the solution was carefully removed, the cell was rinsed with PBS for four times to remove $K_4Fe(CN)_6$ remaining in the tip-substrate gap. Finally, sample solution was added into the electrolytic cell, a steady potential was applied on the tip electrode, and the current–time curves were recorded. A break of 5 min was used between each measurement of current–time curves.

2.3. Immobilization of GOD on substrate electrode

GOD was co-immobilized with a layer of poly-PPD on the GCE based on a procedure described previously (Xu and Chen, 2000). Briefly, 25 mg GOD was dissolved in 1 ml PBS (pH 7.4) containing 10 mM PPD. This mixed solution of GOD and PPD was electrochemically polymerized at 0.4 V for 600 s. GOD has an isoelectric point of 4.2, it should be negatively charged in a solution of pH 7.4. It is reported that poly-PPD is positively charged in the same solution. Therefore, GOD can be incorporated into the polymer matrix as a counterion based on electroneutralization principle. The poly-PPD–GOD-modified GCE (P–G–G) was then rinsed with deionized water carefully and potentially scanned between 0.0 and 0.8 V in PBS for 20 cycles to remove the unreacted PPD monomer. Then the modified substrate electrode was immersed in PBS at 4 °C for 12 h before use.

3. Results and discussion

3.1. Characterization of the P–G–G electrode

Scanning electron microscopy (SEM) was used to investigate the surface morphology of the prepared poly-PPD–GOD membrane (Fig. 2). The membrane was of porous structure with average pore size of ca. 200 nm

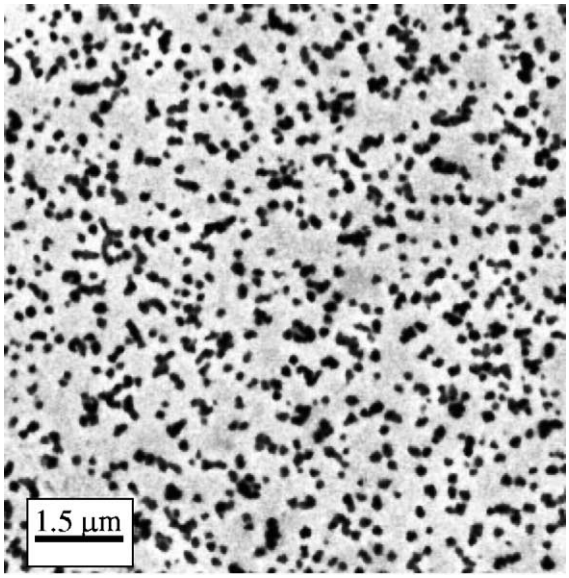

Fig. 2. SEM image of the poly-PPD–GOD membrane.

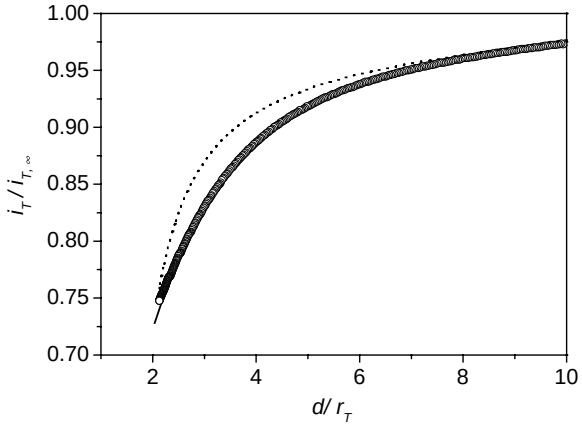

Fig. 3. Normalized current–distance curves recorded with a Pt UME (r_T = 5 μm) in a solution of 1 mM $K_4Fe(CN)_6$ (solid curve) or in a solution of 1 mM $K_4Fe(CN)_6$ + 50 mM glucose (dotted curve). Open circles denote the theoretically calculated current-distance behavior for an insulating substrate.

(dark dots). In addition, the thickness of the membrane was estimated to be 10 μm, using an optical microscopy.

The conductivity and the catalytic reactivity of the obtained P–G–G electrode were characterized using SECM by measuring approaching curves in a $Fe(CN)_6^{4-}$ solution with or without glucose. The tip current and the distance were normalized by $i_{T,\infty}$ (in Eq. (2)) and r_T, respectively. The normalized current–distance curves are shown in Fig. 3. The tip current presented a "negative feedback" (decrease in tip current) behavior at all tip-substrate distances (solid curve) when glucose was absent in solution. This curve fitted well to the theoretically calculated one based on negative feedback for pure insulator (open cycles) (Amphlett and Denuault, 1998). Obviously, the poly-PPD–GOD membrane is a non-conductive system and $Fe(CN)_6^{3-}$ generated on the tip electrode can not penetrate this membrane. The observed pure negative feedback provided us with a direct estimation of the tip-substrate distance (the distance is relative to the top surface of GOD layer). On the contrast, with addition of 50 mM glucose into the solution, the approaching curve (dotted curve) showed an increase in the normalized tip current within short tip-substrate distance. This increase was due to the reduction of the tip-generated ferricyanide via the enzymatic reaction, representing an additional source of ferrocyanide in close proximity to the substrate electrode (Kranz et al., 1997). Obviously, the heterogeneous electron-transfer kinetics between ferricyanide and GOD reaction is relatively slow (Pierce et al., 1992).

3.2. Detection of glucose in the diffusion layer of P–G–G electrode

As H_2O_2 generated on the poly-PPD–GOD would diffuse through the tip-substrate gap before it was detected by the tip electrode, the concentration gradient of H_2O_2 in the solution should be taken into account. In this case, the tip

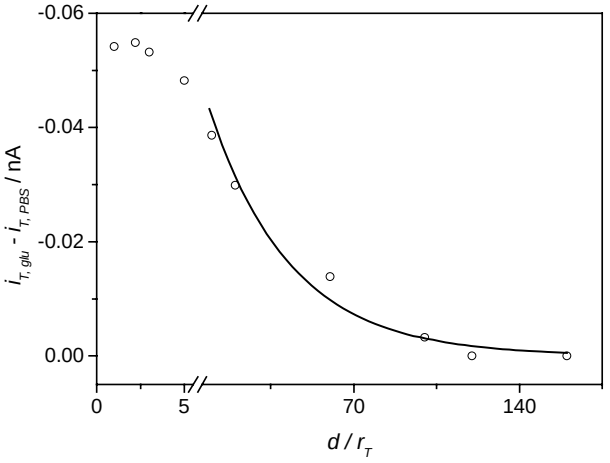

Fig. 4. Dependence of the Pt tip currents ($r_T = 5\,\mu m$, $E_T = 700\,mV$) on the tip-substrate distance in PBS containing 0.1 mM glucose.

current depended on the tip-substrate distance. Meanwhile, diffusion of glucose and generated H_2O_2 from the outside (bulk) to the tip-substrate gap will be restricted when the gap distance is small. This means that the distance between the UME and the P–G–G surface is very critical for the proposed measurement. Therefore, glucose was first detected using the tip electrode in solution without AA at different tip-substrate distances. As show in Fig. 4, the difference between the tip current in 0.1 mM glucose ($i_{T,glu}$) and the tip currents in a buffer solution ($i_{T,PBS}$) drops exponentially with the increase of the normalized tip-substrate distance (d/r_T) in a range of 5 (25 μm) to 120 (600 μm). When the normalized tip-substrate distance was lager than 120, no H_2O_2 could be detected. When the tip-substrate distance was in the range of 2.2 r_T (11 μm) and 5 r_T (25 μm), the tip current became less sensitive to the change of tip-substrate distance. This demonstrates that measurement of glucose in this relatively large range can give reproducible signal even with slight change of tip-substrate distance. When the tip-substrate distance is much shorter (1 r_T, 5 μm), an inhibition of the diffusion of glucose induced by the tip electrode emerges, resulting in a little decrease of the tip current.

At optimized tip-substrate distance (2.2 r_T), the amperometric dynamic responses of the tip electrode to glucose were measured in different glucose concentrations (Fig. 5, inset). After a potential was applied to the tip electrode, the tip current dropped significantly in the first 2 s due to the rapid decrease of charging current and the depletion of the previously accumulated H_2O_2 in the tip-substrate gap formed via enzymatic reaction (Eq. (1)). Then the tip current reached a relative steady state value when the diffusion of H_2O_2 from the outside of the tip-substrate gap was equal to the consumption of H_2O_2 on the tip electrode. Steady-state tip currents taken at the polarization time of 5 s increase linearly (Fig. 5) with the concentration of glucose in the range of 0.01–1 mM (correlation coefficient: 0.9994) with a detection limit (DL) of 0.005 mM. In more concentrated glucose solutions, the tip currents deviated from the linearity owing to the change of the enzymatic reaction kinetics from first order at low glucose concentration (<1 mM) to zero order at high glucose concentration (>4 mM).

3.3. Interference-removing by applying oxidizing potential on the substrate electrode

As shown in Fig. 6, electrochemical oxidation of AA on both platinum tip (Fig. 6a) and GCE (Fig. 6b) started at more negative potentials (anodic current can be seen at 0.0 V, solid

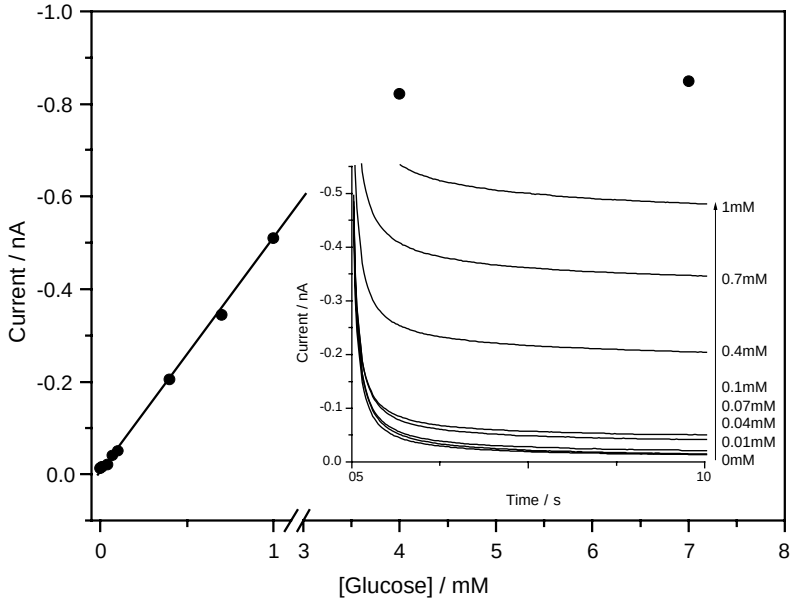

Fig. 5. Response currents of the tip electrode taken at the polarization time of 5 s as a function of glucose concentration. Inset denotes the current responses of the tip electrode ($r_T = 5\,\mu m$) at 0.7 V for different glucose concentrations as a function of time. The tip-substrate separation distance was 11 μm.

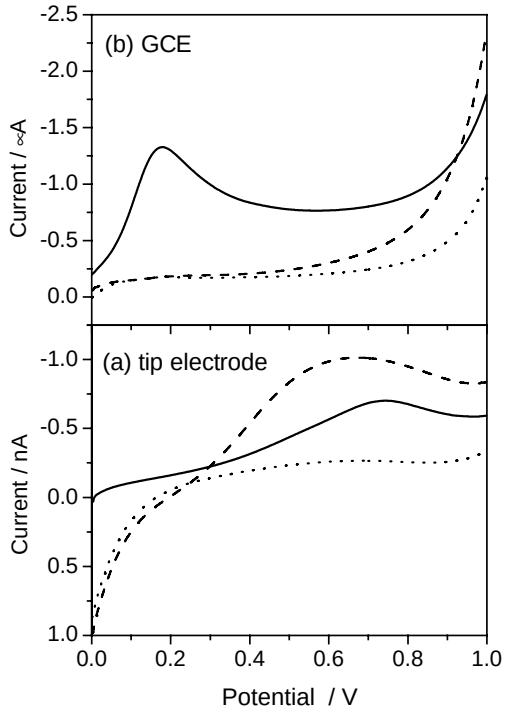

Fig. 6. Voltammograms of a GCE and a Pt UME ($r_T = 5\,\mu m$) in PBS (doted curves) and PBS containing 0.1 mM AA (solid curves) or 0.1 mM H_2O_2 (dashed curves) at a scan rate of 50 mV/s.

curves) than that of H_2O_2 (dashed curves). The difference of the onset potential between AA and H_2O_2 on tip electrode results in an inevitable interfering current during the detection of H_2O_2. In the case of GCE, the oxidation rate of AA reaches diffusion-limited level at potentials more positive than 0.17 V. For the oxidation of H_2O_2 on GCE, no obvious anodic current appeared at potential lower than 0.5 V. Thus, by controlling the substrate electrode potential between the anodic peak potential of AA (0.2 V) and the potential for the electro-oxidation of H_2O_2 (0.5 V), AA in the diffusion layer of the GCE could be successfully depleted irreversibly without consumption of H_2O_2.

The influence of substrate potential on the removal of interference and detection of glucose was investigated at a fixed tip-substrate distance of 11 μm with the tip potential set at 0.5 or 0.7 V. Tip currents with ($i_{T,S}$) and without ($i_{T,0}$) applying a substrate potential were measured, respectively. In the solution of AA, the ratio of $i_{T,S}/i_{T,0}$ represents the percentage of AA in the tip-substrate gap which had not been consumed by the substrate electrode. Therefore, this current ratio could be used to evaluate the interference-removing efficiency of the present design. Here, we define $1-i_{T,S}/i_{T,0}$ as the interference-removing efficiency. A lower ratio means a higher interference-removing efficiency accordingly. When measurements were performed in glucose solution, this ratio represents the percentage of H_2O_2 in the tip-substrate gap that was not consumed by the substrate electrode. Under this circumstance, $i_{T,S}/i_{T,0}$ was used to evaluate the influence of substrate potential on glucose detection. As shown

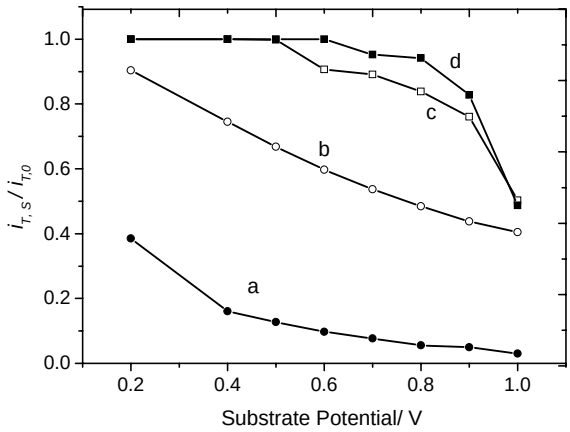

Fig. 7. Dependence of the normalized currents of a Pt tip electrode ($r_T = 5\,\mu m$) at 0.5 V (curves 'a' and 'd') and 0.7 V (curves 'b' and 'c') on the substrate potential. The tip-substrate distance is kept at 2.2 r_T (11 μm) and the tip currents were taken at the polarization time of 30 s. The tip current of $i_{T,0}$ was measured with the substrate electrode at open-circuit potential. 'a': 0.5 mM AA, $E_T = 0.5$ V; 'b': 0.5 mM AA, $E_T = 0.7$ V; 'c': 0.5 mM glucose, $E_T = 0.7$ V; 'd': 0.5 mM glucose, $E_T = 0.5$ V.

in Fig. 7, curves 'a' and 'd' were measured at tip potential of 0.5 V and curves 'b' and 'c' at tip potential of 0.7 V, respectively. In a solution containing 0.5 mM AA (Fig. 7, curves 'a' and 'b'), the tip current ratio decreased with the increase of substrate potential, indicating that a better interference-removing efficiency of the glucose-detecting configuration could be achieved with more positive substrate potentials. However, concerning the detection of glucose (Fig. 7, curves 'c' and 'd'), the tip current ratio decreased gradually with the substrate potential higher than 0.5 V due to partial oxidation of generated H_2O_2 at the substrate electrode. Furthermore, for AA solutions, the observation that tip currents ratio at tip potential of 0.7 V (Fig. 7, curve 'b') is higher than that of 0.5 V (Fig. 7, curve 'a') indicates that lower tip potential should be taken for the precise determination of glucose in a solution containing AA. When both the tip and substrate potentials were set at 0.5 V, most AA (nearly 90% percent) in the tip-substrate gap was eliminated.

The influence of the tip-substrate distance on the interference-removing capability was studied in a solution of 0.5 mM AA with ($i_{T,S}$) or without ($i_{T,0}$) applying 0.5 V on the substrate electrode. Ratios of $i_{T,S}$ to $i_{T,0}$ ($i_{T,S}/i_{T,0}$) as the function of the normalized tip-substrate distance are shown in Fig. 8. The almost linear decrease of the ratio with the normalized tip-substrate distance indicates that the interference-removing efficiency increases with the decrease of tip-substrate distance. Within the tip-substrate distance of 6 r_T (30 μm), the interference-removing efficiency is higher than 80%. With the tip-substrate distance shorter than 2.2 r_T (11 μm), $i_{T,S}/i_{T,0}$ reaches a relatively steady value of about 10% (the interference-removing efficiency is nearly 90%). This demonstrates that measurements in a relatively large tip-substrate distance range (within 6 r_T) could give a stable and high interference-removing efficiency.

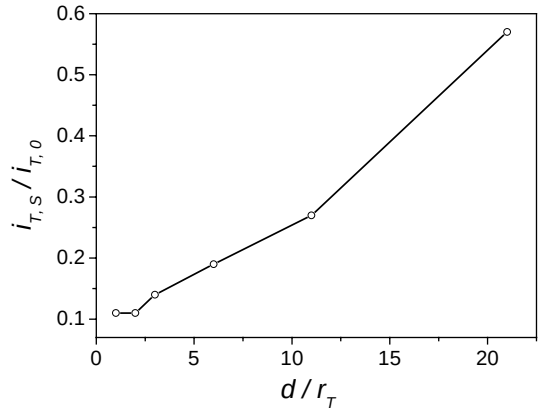

Fig. 8. Dependence of the normalized response current in 0.5 mM AA on the normalized tip-substrate distance. Tip currents were measured with ($i_{T,S}$) or without ($i_{T,0}$) applying 0.5 V on the substrate electrode (E_T = 0.5 V).

Fig. 9 shows the amperometric dynamic responses of the tip electrode in solutions of 0.5 mM glucose with (Fig. 9, curve 'b') or without 0.1 mM AA (Fig. 9, curve 'c') measured under optimized conditions. In a primary research we found that, in a buffer solution with or without glucose, the oxidation potential applied on the substrate electrode (0.5 V) has no influence on the tip current (data not shown due to the complete overlap of tip currents). For comparison, the tip currents in the solution of 0.5 mM glucose with 0.1 mM AA (Fig. 9, curve 'a') were also measured without applying a substrate potential. The tip current shown in curve 'a' is about 2.5 times higher than that in curve 'c', indicating that AA seriously interferes glucose detection without electrochemical depletion. When an oxidation potential of 0.5 V was applied on the substrate electrode (curve 'b'), the tip current decreased dramatically. In the first 20 s of the polarization time, the tip current in curve 'c' is obviously larger than that in curve 'c'. The increased tip current is due to the interference from the electrooxidation of AA, since AA is not yet completely depleted by both electrodes. However, overlap of these two curves at polarization time longer than 25 s indicates that the concentration of AA remaining in the tip-substrate gap in this time period is negligible. Under optimal conditions for interference removing, the linear range of glucose detection is 0.01–1.0 mM with a correlation coefficient of 0.9948 (DL = 0.005 mM).

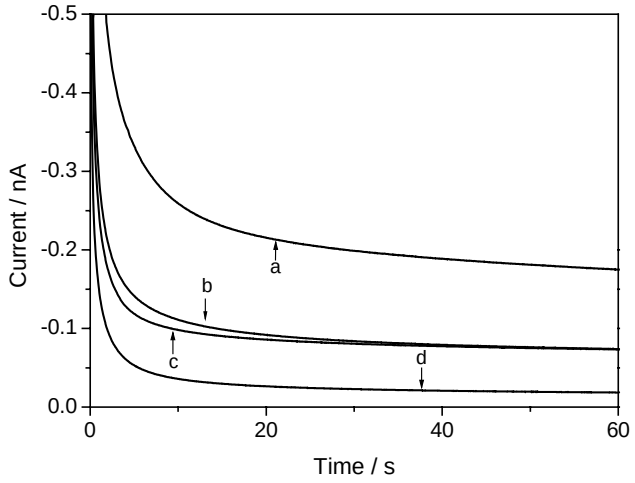

Fig. 9. Amperometric dynamic response of a Pt tip electrode (r_T = 5 μm, E_T = 0.5 V) with and without applying an oxidation potential to the substrate electrode. Tip-substrate distance was kept at 11 μm. 'a': 0.1 mM AA + 0.5 mM glucose, substrate electrode at open circuit potential; 'b': 0.1 mM AA + 0.5 mM glucose, E_{sub} = 0.5 V; 'c': 0.5 mM glucose, E_{sub} = 0.5 V; 'd': PBS supporting electrolyte (pH 7.4), E_{sub} = 0.5 V.

4. Conclusions

This research showed that the diffusion layer of a substrate electrode could be used as an interference-free micro-circumstance for glucose detection using an UME. This glucose detection configuration provides us with a new direction for fabricating interference-free biosensors based on the conception of electrochemical depletion of electroactive species in diffusion layer. SECM was a powerful tool for convenient spatial control in this research. For further research, UMEs could be screen-printed at an optimal position in the diffusion layer of a substrate electrode, and a chip-based glucose biosensor could be fabricated, which makes this configuration promising for practical applications.

Acknowledgements

This work was supported by Grants from the National Natural Science Foundation of China (NSFC, No. 20125515; 20299030; 20375016).

References

Amphlett, L.J., Denuault, G., 1998. Scanning electrochemical microscopy (SECM): an investigation of the effects of tip geometry on amperometric tip response. J. Phys. Chem. B 102, 9946–9951.

Bard, A.J., Fan, F.R.F., Kwak, J., Lev, O., 1989. Scanning electrochemical microscopy. Introduction and principles. Anal. Chem. 61, 132–138.

Gaspar, S., Mosbach, M., Wallman, L., Laurell, T., Csoregi, E., Schuhmann, W., 2001. A method for the design and study of enzyme microstructures formed by means of a flow-through microdispenser. Anal. Chem. 73, 4254–4261.

Gerard, M., Chaubey, A., Malhotra, B.D., 2002. Application of conducting polymers to biosensors. Biosens. Bioelectron. 17, 345–359.

Kasai, S., Hirano, Y., Motochi, N., Shiku, H., Nishizawa, M., Matsue, T., 2002. Simultaneous detection of uric acid and glucose on a dual-enzyme chip using scanning electrochemical microscopy/scanning chemiluminescence microscopy. Anal. Chim. Acta 458, 263–270.

Kasai, S., Yokota, A., Zhou, H.F., Nishizawa, M., Niwa, K., Onouchi, T., Matsue, T., 2000. Immunoassay of the MRSA-related toxic protein, leukocidin, with scanning electrochemical microscopy. Anal. Chem. 72, 5761–5765.

Kranz, C., Wittstock, G., Wohlschlager, H., Schuhmann, W., 1997. Imaging of microstructured biochemically active surfaces by means of scanning electrochemical microscopy. Electrochim. Acta 42, 3105–3111.

Kwak, J., Bard, A.J., 1989. Scanning electrochemical microscopy. Apparatus and two-dimensional scans of conductive and insulating substrates. Anal. Chem. 61, 1794–1799.

Kwak, J., Bard, A.J., 1989. Scanning electrochemical microscopy. Theory of the feedback mode. Anal. Chem. 61, 1221–1227.

Liebetrau, J.M., Miller, H.M., Baur, J.E., 2003. Scanning electrochemical microscopy of model neurons: imaging and real-time detection of morphological changes. Anal. Chem. 75, 563–571.

Lunte, C.E., Ridgway, T.H., Heineman, W.R., 1987. Voltammetric-amperometric dual-electrode detection for flow injection analysis and liquid chromatography. Anal. Chem. 59, 761–766.

Mello, L.D., Kubota, L.T., 2002. Review of the use of biosensors as analytical tools in the food and drink industries. Food Chem. 77, 237–256.

Myler, S., Collyer, S.D., Bridge, K.A., Higson, S.P.J., 2002. Ultra-thin-polysiloxane-film-composite membranes for the optimisation of amperometric oxidase enzyme electrodes. Biosens. Bioelectron. 17, 35–43.

Pierce, D.T., Unwin, P.R., Bard, A.J., 1992. Scanning electrochemical microscopy. 17. Studies of enzyme-mediator kinetics for membrane- and surface-immobilized glucose oxidase. Anal. Chem. 64, 1795–1804.

Turyan, I., Matsue, T., Mandler, D., 2000. Patterning and characterization of surfaces with organic and biological molecules by the scanning electrochemical microscope. Anal. Chem. 72, 3431–3435.

Wang, J., 2001. Glucose biosensors: 40 years of advances and challenges. Electroanalysis 13 (12), 983–988.

Xiao, Y., Patolsky, F., Katz, E., Hainfeld, J.F., Willner, I., 2003. Plugging into enzymes: nanowiring of redox enzymes by a gold nanoparticle. Science 299, 1877–1881.

Xu, J.J., Chen, H.Y., 2000. Amperometric glucose sensor based on coimmobilization of glucose oxidase and poly(*p*-phenylenediamine) at a platinum microdisk electrode. Anal. Biochem. 280, 221–226.

Zhang, Y., Hu, Y., Wilson, G.S., Moatti-Sirat, D., Poitout, V., Reach, G., 1994. Elimination of the acetaminophen interference in an implantable glucose sensor. Anal. Chem. 66, 1183–1188.

Zhou, J.F., Campbell, C., Heller, A., Bard, A.J., 2002. Scanning electrochemical microscopy. 44. Imaging of horseradish peroxidase immobilized on insulating substrates. Anal. Chem. 74, 4007–4010.